Spectroscopic investigation of the equilibrium state in the electric arc cathode region

1996 J. Phys. D: Appl. Phys. 29 2644

(http://iopscience.iop.org/0022-3727/29/10/015)

J. Phys. D: Appl. Phys. **29** (1996) 2644–2649. Printed in the UK

Spectroscopic investigation of the equilibrium state in the electric arc cathode region

B Pokrzywka†, K Musioł‡, S Pellerin§, E Pawelec‡ and J Chapelle§

† Institute of Physics, Cracow Pedagogical University, ul. Podchorążych 2, 30-084 Kraków, Poland
‡ Institute of Physics, Jagellonian University, ul. Reymonta 4, 30-459 Kraków, Poland
§ GREMI, Université d'Orléans, BP 6759, 45067 Orléans Cedex 2, France

Received 5 February 1996, in final form 7 May 1996

Abstract. Several thin layers of an arc plasma column were observed side-on at different distances from the cathode. The arc was operated in argon at atmospheric pressure with the arc current equal to 200 A. As the basic diagnostic method we used the Olsen–Richter diagrams. For determination of temperature the Larenz–Fowler–Milne and Boltzmann plot methods were applied. Electron density was measured from the Stark width of the ArII line and continuum intensity.

The plasma near the cathode tip shows axial and radial dependence of its physical equilibrium state. In the hot core, the plasma is in LTE. Toward outer zones, the plasma state deviates from LTE. For plasma layers closer to the cathode, this deviation begins at smaller distances from the axis and for higher temperatures it vanishes for $h > 3$ mm. It is caused after all by the ArI ground state overpopulation. Theoretical estimations of the ArI ground state overpopulation give results consistent with experiment. Calculations show that this overpopulation is caused by inward transport of ground state atoms into the plasma column.

1. Introduction

The near cathode zone of an electric arc has been intensively studied over recent years. For arcs working at atmospheric pressure, with a current of few hundred amperes, at distances from the cathode of less than 4.5 mm, the total intensity radial distribution of the neutral atom line shows an off-axis maximum (norm intensity). For plasmas in local thermodynamic equilibrium (LTE) and constant pressure, the norm intensity is reached for one temperature value—the norm temperature. It has already been observed in several experiments that this off-axis maximum value depends on the distance from the cathode and has been reported by Haddad and Farmer [1], Haidar and Farmer [2, 3], Razafinimanana *et al* [4], in our previous experiments [5, 6] for argon and by Haidar and Farmer [7] and Megy *et al* [8, 9] in nitrogen.

Two explanations are possible. Either the plasma equilibrium state depends on the distance from the cathode or pressure gradients exist in the investigated plasma zone.

In our previous publications [5, 6] we presented results of spectroscopic diagnostics performed for an argon arc plasma at atmospheric pressure with arc current of 200 A where these phenomena were observed. In the present paper results of similar experiments but with an improved experimental set-up and better spectroscopic plasma diagnostics are described. In the new experiment we intended to avoid the most important shortcomings encountered previously. The continuum radiation intensity and ArIII spectral lines were added in the new experiment to the list of spectroscopic measurements. We were also able to construct two Olsen–Richter (OR) graphs for the same plasma layers using spectral lines emitted by argon in three consecutive ionization stages.

It was reported by Razafinimanana *et al* [4] (for argon) and by Megy *et al* [8, 9] (for nitrogen) that close to the cathode, the free electron density derived from the continuum radiation intensity was not consistent with that obtained from other spectroscopic methods. In order to find a reason for these discrepancies and to check the consistency of results from different diagnostic techniques we decided to measure the continuum radiation at $\lambda = 468.8$ nm. From the radial distribution of continuum intensity, we were able to construct the OR diagram using the emission coefficients for the continuum radiation and 480.6 nm ArII line. In order to find which mechanism plays the dominant role in the phenomenon described above, we also performed plasma model calculations.

0022-3727/96/102644+06$19.50

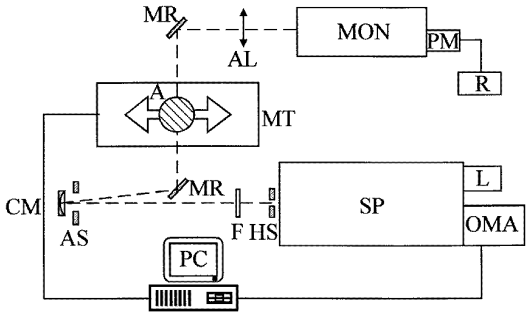

Figure 1. Experimental set-up: SP, spectrometer; OMA, OMA III optical multichannel analyser; L, He–Ne laser; HS, horizontal slit; F filter; AS, aperture stop; CM, concave mirror; MR flat mirror; MT, step motor driven X–Z movable table; A, plasma source; AL, achromatic lens; MON, monochromator; PM, photomultiplier; R, recorder; PC, computer.

2. Experimental set-up

A schematic of the apparatus used in our experiments is shown in figure 1. Study of the arc column between the cathode and first disc was performed side-on. Several thin layers of the plasma column were observed at different distances from the cathode tip ($0 > h > 4.5$ mm).

2.1. Plasma source

The applied arc is shown in figure 2. The sharpened rod of 4 mm diameter, made of 2% thoriated tungsten, was fixed in a water-cooled copper cone having a 40° conical angle. The gas had small axial velocity and aspired to the plasma column mainly due to the Maecker effect [10]. The upper part of the arc consisted of three copper disks with a 5 mm diameter channel in the centre. The third disc worked as an anode. The first two stabilizing disks permitted isolation of the cathode region from the influence of the anode. The arc was placed in a chamber connected to the pressure control system. Before arc ignition, air was pumped out from the chamber. Then, the argon flow was set to a small value (about 0.1 l h^{-1}) to keep pressure in the chamber close to 4 mbar. The discharge was started by a short high-voltage pulse. After breakdown, pressure in the chamber was rapidly raised to slightly above atmospheric. In this way the chamber protected the entire plasma volume from diffusion of air very well. The arc was operated with a pure argon (purity better than 99.995%) flow of $d_g = 2.0$ l min^{-1} and the arc current I_{arc} was 200 A. The chamber was mounted on an X–Z translation stage whose motion in the horizontal direction was realized by a step motor controlled by the on-line computer.

2.2. Acquisition system and experimental procedure

The plasma column was imaged onto the entrance slit of an Ebert-type spectrometer by a system of mirrors. An additional horizontal slit reduced the thickness of the observed plasma column layer to 25 μm. The entrance slit of the monochromator was set to 25 μm. The magnification factor and aperture were 1 and 1:140 respectively. The spectrometer worked in the second diffraction order with resolution of 150 000 and reciprocal dispersion of 0.2 nm mm^{-1}.

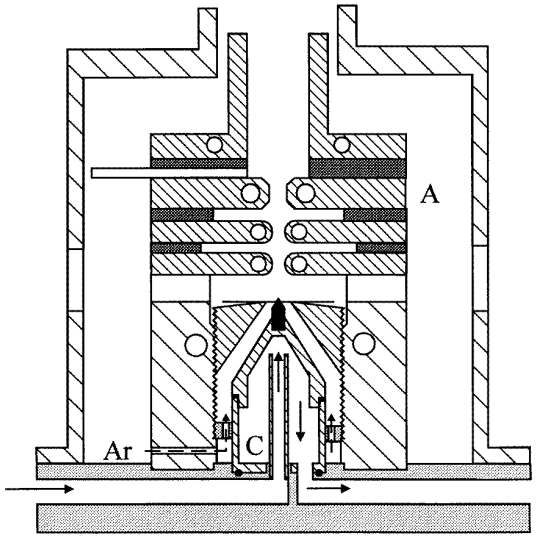

Figure 2. Plasma source: A, anode; C, cathode.

An optical multichannel analyser (OMA III), equipped with a linear photodiode array coupled with an image intensifier, having 800 intensified pixels (25 $\mu\text{m} \times 2.5$ mm), was used as the light detector. The photodiode array simultaneously registered about 4 nm of the spectrum, thus the line profiles were measured up to their far wings. All apparatus factors—such as apparatus profile, spectrometer dispersion, dark current detector signal, its linearity, flat fielding and stability—were determined or checked.

A He–Ne laser, fixed in the spectrometer dispersion plane, allowed alignment of the optical system and measurement of slit width. The laser beam was also used to determine the position of the observed column layer and its distance from the cathode tip. A second optical system was used to control plasma stability by recording the 480.6 nm ArII total line intensity. The arc current and voltage were also registered during the experiment.

3. Data treatment and analysis

The measured spectral lines and their most important parameters are presented in table 1. The side-on measured spectral line intensity distribution was converted into the radial distribution of the emission coefficient pixel by pixel, using the Abel inversion procedure. Inversion was performed for 96 horizontal arc positions and 200 to 700 pixels depending on the spectral line width under study. Among many methods of the Abel inversion, the method based on cubic spline data smoothing was chosen [11]. After the inversion, the Voigt function with a linear continuous background was fitted to experimental line profiles. Total line intensities were calculated using fitted parameters values, thus the spectral line wings were automatically included.

Table 1. Measured spectral lines and their parameters.

λ(nm)	Element	Upper level	Lower level	E_g (eV)	E_d (eV)
696.54	ArI	$4p[\frac{1}{2}]_1$	$4s[\frac{1}{2}]_2$	13.33	11.55
480.6	ArII	$4p^4P^0_{5/2}$	$4s^4P_{5/2}$	19.22	16.64
397.9	ArII	$4d^4P^0_{1/2}$	$4p^4S^0_{3/2}$	23.08	19.97
396.84	ArII	$4p^4D^0_{5/2}$	$3d^4D_{5/2}$	19.55	16.42
397.47	ArII	$4p^2D^0_{3/2}$	$4s^4P_{5/2}$	19.76	16.64
397.45	ArII	$4p^2P^0_{3/2}$	$4s^4P^0_{3/2}$	19.87	16.75
395.84	ArII	$4d^4D_{3/2}$	$4p^2P^0_{5/2}$	22.81	19.68
398.82	ArII	$4d^4D_{5/2}$	$4p^2D^0_{5/2}$	22.79	19.68
328.58	ArIII	$4p^5P_3$	$4s^5S^0_2$	25.36	21.62
330.19	ArIII	$4p^5P_2$	$4s^5S^0_2$	25.37	21.62

Reabsorption analysis and correction was performed by means of the iterative Abel inversion [12], using the Planck distribution as the source function. In each iteration step the temperature and optical depths fields were determined. Then initial chordal intensities were corrected for self absorption and the Abel inversion was repeated with corrected values. For the presented data the correction factor to the total line intensity due to reabsorption never exceeded 5% for the 696.5 nm ArI line, 1.5% for the 480.6 nm ArII and 0.5% for other ArII or ArIII lines.

As a basic plasma diagnostic method the Olsen–Richter (OR) diagram was used [13, 14] which is particularly useful in analysis of the plasma equilibrium state (see [6] for details). It is the log–log plot of total emission coefficients either for two spectral lines emitted by particles in two consecutive ionization stages or for the spectral line and the continuum intensity. For a given pressure, such a dependence may be theoretically calculated using the LTE plasma equation set. If experimental points in the OR graph do not follow the ambient pressure isobar, formally two reasons are possible: either a transition from LTE to partial LTE state (PLTE) occurs or pressure gradients exist in the plasma.

We measured the continuum radiation intensity distribution at $\lambda = 468.8$ nm ($\Delta\lambda = 0.005$ nm) since for this wavelength values of the Biberman ξ factor can be found in the literature. For this wavelength, the ξ factor shows a very weak dependence on the plasma temperature [15]. The continuum radiation emission coefficient ε_{tot} may be described by the following expression:

$$\varepsilon(\lambda, T_e) = C_1 n_e T_e^{-1/2} \sum_{z=1}^{2} n_z z^2 \left\{ \left[1 - \exp\left(-\frac{hc}{\lambda k T_e} \right) \right] \times \frac{g_{z,1}}{U_z(T_e, n_e)} \xi_{fb}(\lambda, T_e, z) + \exp\left(-\frac{hc}{\lambda k T_e} \right) \xi_{ff}(\lambda, T_e, z) \right\}$$

$$C_1 = \frac{16\pi e^6}{3c^2(4\pi\varepsilon_0)^3(6\pi m_e k)^{1/2}}$$

where z denotes the charge of the ion interacting with free electrons, n_e electron density, n_z ions density and g_z and U_z are the statistic weight and partition function respectively. ξ_{ff} and ξ_{fb} are the Biberman factors for free–free and free–bound transitions respectively. The ξ factor for free–bound transitions was taken from the works of Timmermans [16] and Hofsaess [15] and that for free–free transitions from Cabannes and Chapelle [17]. It should be noticed that at temperatures $T \approx 24\,000$ K, ArIII and ArII contributions to the continuum are similar, and the free–free contribution is about 30% of the free–bound contribution.

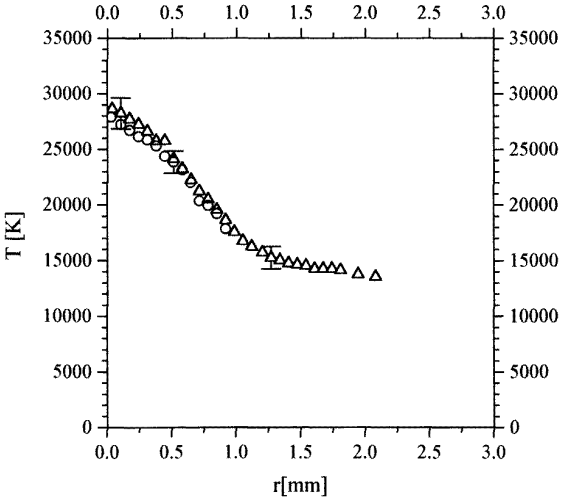

Figure 3. Temperature radial distribution in the layer $h = 0.085$ mm. (○) results from the Boltzmann plot for ArII lines, (△) results from the Larenz–Fowler–Milne method applied to 480.6 nm ArII line. For clarity only typical errors are shown.

4. Results

At distances from the cathode less than 5 mm, the total intensity of the 696.5 nm ArI line exhibited an off-axis maximum. In regions closer than 0.5 mm to the cathode tip the off-axis maximum also appeared for the 480.6 nm and 396.8 nm ArII lines. In this region ArIII lines were also detected [18]. The off-axis maximum value of the 696.5 nm line depended on the distance from the cathode and very close to its surface decreased to about 50% of the highest value, which was reached at a distance of about 3 mm from the cathode. For distances larger that this limit, this off-axis maximum stayed constant, in agreement with previous observations [1, 5, 6].

The norm intensity for ArII lines was independent of the distance from the cathode which permits application of the Larenz–Fowler–Milne (LFM) method for determination of the radial temperature distribution [19, 20]. The radial temperature distribution was also obtained from the Boltzmann plot for ArII lines listed in table 1. The transition probabilities for these lines were taken from the study by Pellerin [21]. We found very good agreement between the temperatures determined from both methods. As an example, the temperature distribution, in the plasma layer at $h = 0.085$ mm is shown in figure 3.

The free electron density, in the plasma region with a temperature above 18 000 K, was determined from the Stark width of the 397.9 nm ArII line profile [21] and compared with values calculated from the LTE equations set for the temperature derived from the Boltzmann plot at $p = 1$ atm.

We found agreement within 5%. These results permit us to conclude that the population distribution of ArII excited levels was in the Boltzmann–Saha equilibrium for T above $\sim 18\,000$ K.

4.1. Olsen–Richter diagrams

For the investigated plasma layers, the measured radial distributions of emission coefficients for the 696.5 nm and 480.6 nm lines were marked as points in the Olsen–Richter diagram. To superpose the experimental values on the theoretical graph, two constants are needed. In our case we assumed that the highest observed value of the off-axis maximum for the 696.5 nm line ($h > 3$ mm) corresponded to its norm intensity for the plasma in the LTE state at atmospheric pressure. Taking into account remarks concerning the Boltzmann–Saha equilibrium for ArII levels described above, the same assumption was made for the norm intensity of 480.6 ArII line. In this way the two necessary constants were determined.

A similar method was applied to construct the OR diagram for another pair of lines: the 330.1 nm ArIII and 480.6 nm ArII line. For this graph, two components of the translation vector in the OR graph should also be determined. However, the calibration constant for the 480.6 nm line had already been determined in the previous graph, thus the superposition of experimental points for ArIII–ArII lines in the OR graph required only one constant. The results of these procedures are shown in figure 4. It can be seen that the experimental data for ArIII and ArII lines can be very well superposed on the curve calculated for the plasma in the LTE state at $p = 1$ atm.

In the OR graph for ArII and ArI lines a good agreement between measured values and the LTE 1 atm isobar is observed only for high temperatures ($T > 17\,000$ K). As the investigated plasma layers approach the cathode tip, disagreement begins to appear for higher temperatures.

Measured values of the continuum radiation emission coefficient at $\lambda = 468.8$ nm were used to trace the third OR diagram, namely for the continuum radiation and 480.6 nm ArII line. The translation constant for the 480.6 nm ArII line was taken from the OR graph described above. The second constant was determined using the continuum intensity experimental points obtained for the temperature range 17 000–18 000 K. In this temperature range, data in the OR graph for ArI–ArII lines lie on the LTE curve (figure 4) and the influence of the ArIII recombination radiation can be neglected. The result of this procedure is shown in figure 5.

For temperatures below 17 000 K there is a good agreement between the experimental data shown in figure 5 and the OR graph for ArI–ArII lines (figure 4). In both graphs results for a plasma layer at a distance 4.5 mm from the cathode follow the LTE 1 atm isobar. For other layers, continuum emission data deviate from the LTE 1 atm isobar in the same manner as the experimental data in the OR graph for ArI–ArII lines.

The deviation for temperatures above 19 000 K observed in figure 5 can be explained as the result of underestimation of the Biberman ξ factor for ArIII

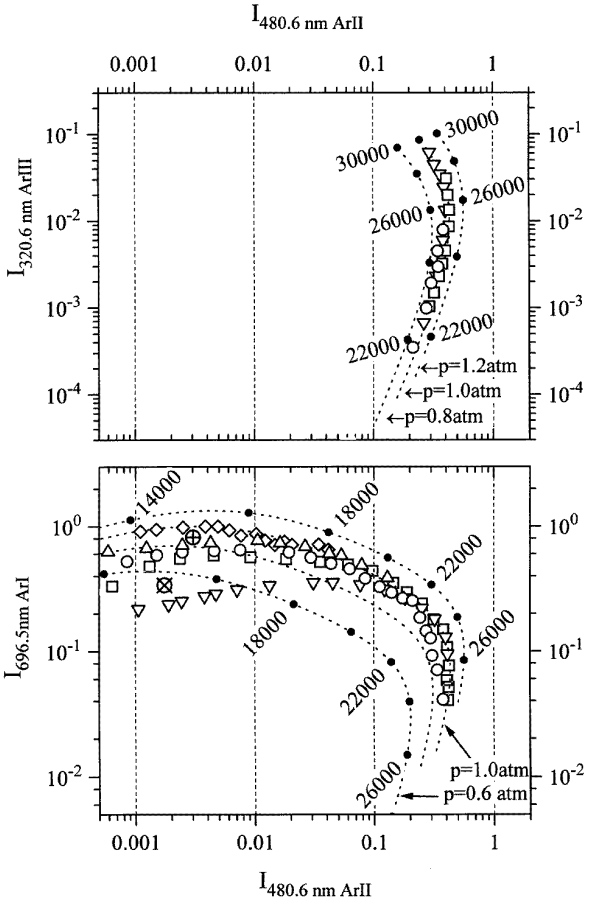

Figure 4. Pair of Olsen–Richter diagrams for the plasma layers at different distances h from the cathode tip. The same symbols and same scale for ArII line are used in both plots. (– – –) LTE isobars with 0.25 atm step, (●) temperature marks on appropriate curve with 2000 K increments. Calculated values for T = 15 000 K: (⊗) h = 0.1 mm, (⊕) h = 0.93 mm (for details see section 5). Experimental points: (▽) h = 0.085 mm, (□) h = 0.51 mm, (○) h = 1.1 mm, (△) h = 2.1 mm (◊) h = 4.5 mm. For clarity only every fourth point is shown.

recombination radiation. This hypothesis is supported by good agreement between the electron density derived from the ArII lines intensity ratio measurement (Boltzmann plot) and the electron density obtained from ArII line broadening measurements. Since the Stark width of spectral lines practically depends only on electron density and does not depend on the plasma state, this conclusion is fairly well justified.

5. Model calculations

In emission spectroscopy it is not possible to determine whether experimental points in the OR graph step aside from the 1 atm isobar because ground state overpopulation or a pressure gradient exists in the plasma. Theoretical analysis may help to find arguments favouring one of these two possibilities. The plasma near the cathode has a conical shape and the well known Maecker effect [10] produces a strong flow of the cold gas from the outer, low-temperature

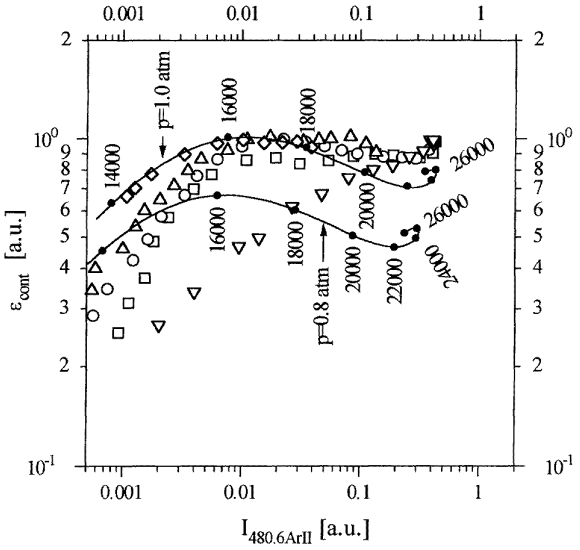

Figure 5. The Olsen–Richter diagram for continuum radiation at λ = 468.8 nm and 480.6 nm ArII line for different distances from the cathode tip. (- - - -) LTE isobars. For experimental points the same symbols and scale for the ArII line are used as in figure 4. In the graph every second point is shown.

parts of the arc towards the axis. The cold gas, composed of atoms in the ground state, cannot reach LTE immediately.

Deviation from LTE may be described only in the frame of the collisional–radiative model. One has to solve the equation set describing the populations of neutral argon states up to the effective ionization limit. In the case of argon plasma at atmospheric pressure, the transport of radiation may be described locally using so-called escape coefficients. The equation set, giving the population of the argon states, may be written for a steady state in the following form:

$$\begin{aligned}\nabla\cdot(\boldsymbol{w}_q n_q) &= n_e\sum_{p=1}^{q-1}(n_p k_{pq}-n_q k_{qp})\\ &-n_e\sum_{p=q+1}^{N}(n_q k_{qp}-n_p k_{pq})+n_e n_q k_{q+}+n_e^2 n_{1+}k_{+q}^{(3)}\\ &+n_e n_{1+}k_{+q}^{(2)}\Lambda_{+q}^{(2)}\\ &-\sum_{p=1}^{q-1}n_q A_{qp}\Lambda_{qp}+\sum_{p=q+1}^{N}n_p A_{pq}\Lambda_{pq}\end{aligned}\qquad(1)$$

where $\boldsymbol{w}_q$ is the drift velocity of atoms in the q state, n_q the density of atoms in the q state, n_{1+} represents ions density in the ground state, n_e the free electron density, k_{qp} the rate coefficient for excitation by electronic collisions from the q to p state, k_{q+} the rate coefficient for ionization by electronic collisions, $k_{+q}^{(3)}$ the rate coefficient for three-body electronic recombination, $k_{+q}^{(2)}$ the rate coefficient for two-body electron recombination, $\Lambda_{+q}^{(2)}$ the escape factor for two-body electronic recombination and A_{pq} and Λ_{pq} are the transition probability and escape factor for transition from p to q state ($E_p > E_q$) respectively.

The solution of this equation set is very difficult, thus in calculation (or rather estimation) of populations we made several simplifications following Rosado [22]. We assumed that the system of argon energy levels can be represented by four effective levels. The first effective state ($q = 1$) is the ArI ground level, the second one is formed by ArI 4s states, the third one ($q = 3$) is formed by ArI 4p levels and the last effective state ($q = 4$) is composed of ArI 5s and 3d states. Each effective state is described by four effective parameters E_q, g_q, A_{qp}, k_{qp}. All these quantities were taken from the work of Rosado [22], where this approach and the calculation method are discussed in detail.

It is more convenient to refer the real population in the q state (n_q) to the population when the Saha equilibrium exists between the q and ionic ground state (n_q^S) and to use the overpopulation factor $\delta_q = (n_q/n_q^S)-1$ and the transport term $W_q = 1/n_q^S\nabla\cdot(\boldsymbol{w}_q n_q)$. We studied the solution of equation (1) for several temperatures between 12 000 K–16 000 K. Overpopulation factors for excited states ($q > 1$) are of the order of 10^{-3} to 10^{-4}. They remain negligible in comparison to δ_1. As could be expected, the dominant effect is the ArI ground state overpopulation, due to the ground state atoms transport term W_1. This overpopulation derived from the OR graph needs the transport term W_1 to be of the order 10^4 to 10^6 s^{-1}, while thermal and ambipolar diffusion can create a value of W_1 about two orders of magnitude lower in our experimental conditions [22]. Thus, inward transport of the ground state ArI atoms should have another origin than diffusion.

We received from Lowke [23] results of his model calculation, performed at our request, for the arc plasma used in our experiments. This model, described in [24] (for different experimental conditions to those used here), is based on magneto-hydrodynamic equations and gives distributions of macroscopic plasma parameters (e.g. temperature, pressure and plasma velocity created by Maecker's effect [10]). Although this model assumes the plasma to be in LTE it can be used as an first approximation for the real physical situation. The calculated maximum temperature was equal to 26 450 K, the overpressure due to the magnetic pinch did not exceed 2% of atmospheric pressure. The plasma velocity in the vicinity of the cathode reached 430 m s^{-1}, showed a strong radial dependence and had a large radial component. The maximum radial velocity was equal to 160 m s^{-1}. This means that there was a strong flow of cold gas from the outer parts of the arc towards the axis.

In order to compare our calculations with experimental data, we calculated W_1 and δ_1 for two points on the 15 000 K isotherm using the temperature and velocity distributions calculated by Lowke [23]. Atoms and free electron density distributions were calculated for this temperature, using simultaneously the PLTE equation set and equation (1).

For $h = 0.1$ mm and $T = 15\,000$ K, we obtained W_1 values as high as -5×10^5 s^{-1}, which produces the ground state overpopulation $\delta_1 \approx 5$. This overpopulation 'locates' the corresponding point in the OR diagram on the LTE isobar for $p = 0.5$ atm and gives an electron density 42% lower than the LTE value.

For $h = 0.93$ mm and $T = 15\,000$ K, we obtained $W_1 \approx -5\times10^4$ s^{-1} and $\delta_1 \approx 0.53$. These values correspond

to the LTE plasma composition for $p = 0.86$ atm. For the same plasma layer, at the radial distance where $T = 12\,000$ K, we obtained $W_1 \approx -5.7 \times 10^3$ s^{-1} and $\delta_1 \approx 1.3$, which is equivalent to LTE pressure of 0.55 atm. It can be seen from figure 4 that these estimations are in good qualitative agreement with our experimental results presented in the OR graph. The presented model allows us to explain the behaviour of the neutral argon spectral line intensity distribution.

6. Conclusions

From our analysis one can conclude the following.

(i) The off-axis maximum value of the 696.5 nm line depended on the distance from the cathode and very close to its surface it decreased to about 50% of the highest (norm intensity) value.

(ii) The population distribution of ArII excited levels was in Boltzmann–Saha equilibrium for T above $\sim$17 000 K. This conclusion is justified by a very good agreement between the temperatures determined from the Boltzmann plot and the LFM method applied to the 480.6 nm ArII line.

(iii) The arc plasma near the cathode tip shows a radial dependence of the physical equilibrium state. In the outer zones, the plasma state deviates from LTE at $p = 1$ atm. For plasma column layers (slices) closer to the cathode tip, deviation from the LTE state begins at smaller distances from the axis and for higher temperatures, even if the electron density is greater than 1.5×10^{23} m^{-3}. Deviation from the LTE state decreases with the distance from the cathode and practically vanishes for $h > 3$ mm.

(iv) Continuum radiation for temperatures below $\sim$16 000 K deviates from the LTE isobar in the OR graph in the same manner as the experimental data for ArI–ArII lines. Disagreement observed for temperatures above $\sim$ 19 000 K is in our opinion a result of underestimation of the Biberman ξ factor for ArIII recombination radiation.

(v) From our calculations it can be concluded that overpopulation factors for excited states are of the order 10^{-3} to 10^{-4}. They remain negligible in comparison with the ground state overpopulation factor. The dominant impact on ArI ground state overpopulation is the inward transport of ground state atoms.

Acknowledgments

We thank Professor Lowke for sending us results of his model calculations. This work was supported in equal parts by the Polski Komitet Badan Naukowych (Grant 2P302.05105) and Electricite de France.

References

[1] Haddad G N and Farmer A J 1984 *J. Phys. D: Appl. Phys.* **17** 1189
[2] Haidar J and Farmer A J D 1993 *Proc. XXI ICPIG (Bochum)* p 54
[3] Haidar J and Farmer A J D 1994 *J. Phys. D: Appl. Phys.* **27** 555
[4] Razafinimanana M, Gudzy P, Gleizes A, El Hamidi L and Vacqui S 1994 *J. High Temp. Chem. Proc.* **4** 51
[5] Pellerin S, Musiol K, Pokrzywka B and Chapelle J 1992 *J. High Temp. Chem. Proc Suppl.* **3-1** 478
[6] Pellerin S, Musiol K, Pokrzywka B and Chapelle J 1994 *J. Phys. D: Appl. Phys.* **27** 522
[7] Haidar J and Farmer A J D 1993 *J. Phys. D: Appl. Phys.* **26** 1224
[8] Megy S, Ageorges H, Ershov-Pavlov E A, Sanon A and Baronnet J M 1992 *J. High. Temp. Chem. Proc Suppl.* **3-1** 503
[9] Megy S, Baronnet J M and Ershov-Pavlov E A 1995 *J. Phys. D: Appl. Phys.* **28** 344
[10] Maecker H 1955 *Z. Phys.* **141** 198
[11] Glasser J, Chapelle J and Boetner J 1978 *Appl. Opt.* **17** 23
[12] Griem H R 1964 *Plasma Spectroscopy* (New York: McGraw-Hill) p 179
[13] Richter J 1965 *Z. Astrophys.* **61** 57
[14] Olsen H N 1965 *J. Quant. Spectrosc. Radiat. Transf.* **3** 57
[15] Hofsaess D 1978 *J. Quant. Spectrosc. Radiat. Transf.* **19** 339
[16] Timmermans C J 1984 *Thesis* Eindhoven University of Technology
[17] Cabannes F and Chapelle J C 1971 *Reactions Under Plasma Conditions* ed M Venugopalan (New York: Wiley–Interscience)
[18] Pellerin S, Pokrzywka B, Musiol K and Chapelle J 1995 *J. Physique III* **5** 2029
[19] Fowler R H and Milne E A 1923 *Mon. Not. R. Astron. Soc.* **83** 499
[20] Larentz R W 1955 *Z. Phys.* **129** 198
[21] Pellerin S 1994 *Thesis* University of Orleans, France
[22] Rosado R J 1982 *Thesis* Eindhoven University of Technology
[23] Lowke J J Private communication
[24] Lowke J J, Kovitya P and Schmidt H P 1992 *J. Phys. D: Appl. Phys.* **25** 1601